

AD \_\_\_\_\_

Award Number: DAMD17-03-1-0742

TITLE: Identification of the Molecular Determinants of Breast Epithelial Cell Polarity

PRINCIPAL INVESTIGATOR: Masahiko Itoh, Ph.D.

CONTRACTING ORGANIZATION: University of California  
Berkeley, CA 94720

REPORT DATE: October 2005

TYPE OF REPORT: Annual

PREPARED FOR: U.S. Army Medical Research and Materiel Command  
Fort Detrick, Maryland 21702-5012

DISTRIBUTION STATEMENT: Approved for Public Release;  
Distribution Unlimited

The views, opinions and/or findings contained in this report are those of the author(s) and should not be construed as an official Department of the Army position, policy or decision unless so designated by other documentation.

# REPORT DOCUMENTATION PAGE

Form Approved  
OMB No. 0704-0188

Public reporting burden for this collection of information is estimated to average 1 hour per response, including the time for reviewing instructions, searching existing data sources, gathering and maintaining the data needed, and completing and reviewing this collection of information. Send comments regarding this burden estimate or any other aspect of this collection of information, including suggestions for reducing this burden to Department of Defense, Washington Headquarters Services, Directorate for Information Operations and Reports (0704-0188), 1215 Jefferson Davis Highway, Suite 1204 Arlington, VA 22202-4302. Respondents should be aware that notwithstanding any other provision of law, no person shall be subject to any penalty for failing to comply with a collection of information if it does not display a currently valid OMB control number. **PLEASE DO NOT RETURN YOUR FORM TO THE ABOVE ADDRESS.**

1. REPORT DATE (DD-MM-YYYY) 01-10-2005		2. REPORT TYPE Annual		3. DATES COVERED (From - To) 8 Sep 04 – 7 Sep 05	
4. TITLE AND SUBTITLE Identification of the Molecular Determinants of Breast Epithelial Cell Polarity				5a. CONTRACT NUMBER	
				5b. GRANT NUMBER DAMD17-03-1-0742	
				5c. PROGRAM ELEMENT NUMBER	
6. AUTHOR(S) Masahiko Itoh, Ph.D.  E-Mail: MItoh@lbl.gov				5d. PROJECT NUMBER	
				5e. TASK NUMBER	
				5f. WORK UNIT NUMBER	
7. PERFORMING ORGANIZATION NAME(S) AND ADDRESS(ES)  University of California Berkeley, CA 94720				8. PERFORMING ORGANIZATION REPORT NUMBER	
9. SPONSORING / MONITORING AGENCY NAME(S) AND ADDRESS(ES) U.S. Army Medical Research and Materiel Command Fort Detrick, Maryland 21702-5012				10. SPONSOR/MONITOR'S ACRONYM(S)	
				11. SPONSOR/MONITOR'S REPORT NUMBER(S)	
12. DISTRIBUTION / AVAILABILITY STATEMENT Approved for Public Release; Distribution Unlimited					
13. SUPPLEMENTARY NOTES Original contains color plates: All DTIC reproductions will be in black and white.					
14. ABSTRACT  Establishment of polarity is indispensable for normal glandular function. Conversely, loss of tissue polarity and increased growth are hallmarks of tumorigenesis. Many studies indicate that cell-cell and cell-extracellular matrix interactions are involved in regulation of both cell polarity and growth. Tight junctions, which are the most apical components of cell-cell junctional complexes, play critical roles in the establishment of polarity. However, the molecular pathways that integrate these adhesive interactions to establish tissue polarity remain largely unresolved. A three dimensional laminin-rich extracellular matrix assay system using the HMT-3522 human breast tumor progression series is a good model to address how normal organ structure and function are maintained and how the balance is lost in cancer under physiologically relevant conditions. Using this assay system, I have investigated tight junction components and potential polarity regulator Rap1 which is the Ras superfamily small-G protein. Inhibiting Rap1 in malignant cells induces reversion to polarized acinus-like architecture from disorganized cell clusters. Further activation of Rap1 in malignant cells does not increase colony sizes or proliferation rate compared to control; however, it enhances the resistance for reversion by inhibitors against EGFR or MEK. Rap1 activity also regulates several aspects of malignancy of breast cancer cells.					
15. SUBJECT TERMS No subject terms provided.					
16. SECURITY CLASSIFICATION OF:			17. LIMITATION OF ABSTRACT	18. NUMBER OF PAGES	19a. NAME OF RESPONSIBLE PERSON
a. REPORT U	b. ABSTRACT U	c. THIS PAGE U			USAMRMC
			UU	22	19b. TELEPHONE NUMBER (include area code)

## Table of Contents

<b>Cover.....</b>	<b>1</b>
<b>SF 298.....</b>	<b>2</b>
<b>Table of Contents.....</b>	<b>3</b>
<b>Introduction.....</b>	<b>4</b>
<b>Body.....</b>	<b>4</b>
<b>Reportable Outcomes.....</b>	<b>10</b>
<b>Conclusions.....</b>	<b>10</b>
<b>References.....</b>	<b>10</b>
<b>Appendices.....</b>	<b>12</b>

## **Background**

Multiple cellular processes are dysregulated in tumor formation and progression. Although commonly described as a disease of unrestricted cell proliferation, a defining feature of epithelium-derived cancer is the loss of normal tissue architecture. The finely coordinated integration of a number of processes including cell-cell and cell-ECM interactions, polarity, survival, and proliferation is required for the maintenance of normal tissue architecture. Dysregulation of any of these processes could disrupt tissue organization and lead to tumor formation and progression. Establishment of cell polarity is a fundamental process required for organizing tissue architecture (Itoh and Bissell, 2003). Loss of polarity is often detected as an early event in tumor progression. Thus, determine how molecules and pathways regulate polarity and tissue architecture is crucial for understanding the mechanisms of tumor formation and progression. Recently, three-dimensional (3D) culture systems have received recognition in that they recapitulate features with regard to *in vivo* tissue architecture, and thus provide useful physiologically relevant models for the study of cancer. Our laboratory has been utilizes a 3D laminin-rich extracellular matrix (lrECM) assay system using the HMT-3522 human breast tumor progression series which is comprised of non-malignant S1 cells and malignant T4-2 cells. This is a good model to address how normal organ structure and function are maintained and how the balance is lost in cancer at the molecular level. The purpose of this project is to identify determinants in breast epithelial cell polarity using this model system.

## **Progress**

As I described in the annual report last year, the data obtained from **Task1: Determine which tight junctions components are down/up regulated as human mammary epithelial cells proceed to malignancy** and **Task2: Determine morphological features and localization pattern of tight junction (TJ) components in HMT-3522 series grown in 3D laminin-rich basement membrane with confocal and electron microscopy**, indicated that it would be appropriate to shift the focus slightly to identify molecular mechanisms or pathways that regulate TJ proteins as well as polarity, rather than investigating TJ components themselves in **Task3: Examine gain and loss of function analyses**. Thus, I have examined potential polarity regulator Rap1 which is the Ras superfamily small-G protein in **Task3**. I reasoned that Rap1 could regulate polarity based on the following data;

- 1) Rap1 functions upstream of Erk, PI3K, and Rac1, which are upregulated in malignant T4-2 cells compared to non-malignant S1 cells in 3D lrECM. Reducing the activity of either of these molecules revert disorganized structures of T4-2 cells to organized spheroids.
- 2) Rap1 activity is also increased in T4-2 cells (Figure 1A).
- 3) Rap1 is involved in regulation of integrin-dependent adhesions as well as cadherin-mediated cell-cell adhesions.

To examine gain and loss of function analyses of Rap1, I produced YFP-tagged dominant-active and dominant-negative Rap1 constructs and established stable T4-2 transfectants expressing these constructs (T4-Rap1DA and T4-Rap1DN) as well as YFP as a control (T4-YFP) (Figure 1B). These transfectants were cultured in 3D lrECM to investigate how Rap1 activity affects tissue polarity.

**Inhibiting Rap1 yields a polarized acinus-like structure similar to but distinct from the reverted phenotype by EGFR inhibitor AG1478 in T4-2 cells**

Control T4-YFP cells cultured in 3D lrECM behaved similar to parental T4-2 cells, which proliferated and formed large disorganized colonies (Figure 2A, T4-YFP). In sharp contrast, 3D lrECM cultured T4-Rap1DN cells showed remarkable morphological differences; they formed acinus-like structures similar to non-malignant breast epithelial cells (Figure 2A, T4-Rap1DN). Our lab previously demonstrated that the phenotype of T4-2 cells is altered by the reduction of EGFR activity with EGFR inhibitor AG1478 or inhibitory antibody mAb225 in 3D lrECM (Wang et al., 1998). When control T4-YFP cells were treated with 70nM AG1478, cells underwent growth arrest and formed small organized clusters (Figure 2A, T4-YFP+AG1478). However, spheroids derived from T4-Rap1DN cells differ from AG1478-treated T4-YFP cells in size and organization.

To determine the degree of polarity and the organization of tissue architecture in 3D lrECM cultured transfectants, we examined localization of  $\alpha 6$ -integrin, which is concentrated at basal membrane domains in well-polarized epithelial cells (Figure 2A,  $\alpha 6$ -integrin). In T4-YFP cells,  $\alpha 6$ -integrin was distributed around the entire cell membrane indicating that basal polarity was impaired. On the other hand, polarized localization of  $\alpha 6$ -integrin at the basal membrane domain was observed in T4-Rap1DN and AG1478-treated T4-YFP spheroids. Therefore, basal polarity could be re-established by inhibiting either EGFR or Rap1 signal in T4-2 cells.

I also stained for  $\beta$ -catenin which localizes at basolateral domains and for the apical polarity indicator GM130, a component of the Golgi apparatus, which is distributed at the apical side of the nucleus in polarized cells (Figure 2A,  $\beta$ -catenin and GM130). In T4-YFP colonies,  $\beta$ -catenin was found over the entire cell membrane and GM130 was randomly distributed, indicating that apical and lateral cell polarity was completely disrupted. In T4-Rap1DN spheroids, exclusive concentration of GM130 at the apical side of nucleus and basolateral-restricted distribution of  $\beta$ -catenin was observed, suggesting that expression of dominant-negative Rap1 was sufficient to acquire polarized acinus architecture.  $\beta$ -catenin and GM130 were correctly localized in AG1478-treated T4-YFP cells, but slightly different from those in T4-Rap1DN spheroids.

To compare proliferation kinetics of T4-YFP, T4-Rap1DN, and AG1478-treated T4-YFP colonies, I determined colony sizes and Ki-67 positive ratios at day 3, day 5, and day 8 of culture. At each day the measured T4-Rap1DN spheroids were almost 2-fold larger than AG1478-treated T4-YFP spheroids, while they were 50% smaller than T4-YFP colonies (Figure 2B). The ratio of Ki-67 positive spheroids derived from AG1478-treated T4-YFP cells was significantly decreased at day 5, and only ~5% spheroids were Ki-67 positive at day 8 of culture, indicating that the reversion by treatment with AG1478

seemed to be associated with strong suppression of proliferation. On the other hand, in T4-Rap1DN spheroids, higher Ki-67 positive ratio was maintained till later day of culture and ~ 45% spheroids were Ki-67 positive at day 8.

These results suggested that there was a difference between reversion by inhibiting Rap1 and EGFR signaling, and re-establishment of acinus polarity. Furthermore formation of organized spheroid architecture by expressing dominant-negative Rap1 in malignant T4-2 cells was not simply a consequence of suppressing cell proliferation.

### **Inhibiting Rap1 activity promotes lumen formation by apoptosis in T4-2 cells**

When normal mammary epithelial cells are cultured in 3D lrECM, they proceed through morphogenetic steps to achieve a hollow glandular architecture. During the early steps of morphogenesis (~day 3), apicobasal polarity becomes evident within cell clusters. Around day 6, cells in direct contact with lrECM become well-polarized, whereas cells lacking contact with lrECM are poorly polarized. The cells which are not in contact with lrECM begin to die by apoptosis about day 8 (Debnath et al., 2002).

To investigate whether AG1478-treated T4-YFP and T4-Rap1DN cells follow a similar morphogenesis program, I cultured both cells in 3D lrECM until day 15. AG1478-treated T4-YFP cells showed growth arrest around day 5 and kept almost same condition at day 15. They retained their apicobasal polarity, however, less than 2% spheroids formed a lumen by day 15 (Figure 3A). On the other hand, lumen formation was observed in more than 60% of spheroids derived from T4-Rap1DN cells (Figure 3B). I examined organization of actin-filaments in these cells to compare polarity and confirm lumen formation. The apical localization of actin-filament was detected in T4-Rap1DN cells and not in AG1478-treated T4-YFP cells (Figure 3C).

The immunostaining for the cleaved active-caspase3 at day10 revealed that apoptotic cell death occurred inside of acinus-like structure of T4-Rap1DN cells not contacting with lrECM, whereas it rarely occurred for AG1478-treated T4-YFP cells (Fig. 3D). This result suggested that reversion by inhibiting EGFR signaling alone is not sufficient to activate morphogenetic program of alveolar epithelial cells with apoptotic cell death in 3D lrECM and T4-Rap1DN spheroids had more developed polarity and phenotypically comparable to normal mammary epithelial cells.

### **Dominant-active Rap1 desensitizes T4-2 cells to growth inhibition and re-establishment of polarity by the EGFR inhibitor**

I next investigated the effect of increasing Rap1 activity in acinus architecture of T4-2 cells. When T4-Rap1DA cells were cultured in 3D lrECM, they formed disorganized cellular masses which were indistinguishable from those formed by T4-YFP cells (compare T4-YFP in Figure 2A and T4-Rap1DA in Figure 4A). However, in the presence of normal concentration (70nM) of AG1478, the phenotype of T4-Rap1DA cells was completely different when compared to AG1478-treated T4-YFP cells. T4-Rap1DA cells treated in the same manner with T4-YFP cells continued to proliferate and formed large aggregated colonies similar to untreated cells. In addition, they failed to correctly

localize  $\alpha 6$ -integrin,  $\beta$ -catenin, and GM130. Therefore, T4-2 cells exogenously expressing dominant-active Rap1 acquired resistance to the effect of EGFR inhibitor with regard to the ability to reorganize malignant structures.

In the previous studies, the expression of EGFR and  $\beta 1$ -integrin are correlated with acinus architecture; i.e. these molecules are upregulated in 3D lrECM cultured T4-2 cells compared to S1 cells (Weaver et al., 1997). When T4-2 cells are reverted by inhibiting any of EGFR,  $\beta 1$ -integrin, MEK, or PI3K in 3D lrECM, the expression of EGFR and  $\beta 1$ -integrin are down-regulated while tumor suppressor gene PTEN is up-regulated to levels comparable with those in S1 cells (Liu et al., 2004). Since these changes are not observed in 2D cultures, it is assumed that molecular cross-modulation is associated with tissue architecture. Reverting T4-YFP cells by treatment with 70nM AG1478 resulted in down-regulated expression of both EGFR and  $\beta 1$ -integrin as well as up-regulation of PTEN. However, expression of these molecules was unaffected in T4-Rap1DA cells by the same treatment (Figure 4C).

To investigate if the resistance of dominant-active Rap1 expressing T4-2 cells for inhibitors against EGFR were dose-sensitive or absolute phenotype, I tested higher dose of AG1478 and mAb225 (Figure 5A, B). I also used inhibitors against MEK and PI3K, which have been previously shown to revert malignant phenotype of T4-2 cells, to determine whether active Rap1 affects reversion through these pathways as well (Fig. 5C, D). As shown in Fig. 5C, the same concentration ( $\sim 8\mu\text{M}$ ) of PI3K inhibitor LY294002 was able to revert T4-Rap1DA and T4-YFP cells.

On the other hand, when 210nM AG1478, which was a 3-fold higher concentration than that of required for the reversion of T4-YFP cells, was added to the T4-Rap1DA cells, they were reverted to the non-malignant phenotype (Figure 5A). In a similar way, treatment with an EGFR blocking antibody, mAb225, revealed that 3~4-fold higher dose was required to phenotypically revert T4-Rap1DA cells as compared to T4-YFP controls (Figure 5B). In addition, reversion by inhibiting MEK signaling, 30 $\mu\text{M}$  PD98059 was required for T4-Rap1DA cells, while 10 $\mu\text{M}$  PD98059 was sufficient for T4-YFP cells (Figure 5D).

These results suggested that up-regulation of Rap1 activity affects sensitivity for growth inhibitory signals modulating EGFR-MAPK pathways, and thus could lead to exaggeration of malignant phenotype of T4-2 cells.

### **Rap1 activity affects invasive phenotype and tumorigenesis of T4-2 cells**

I examined if the activity of Rap1 influences other aspects of malignant phenotype of T4-2 cells in addition to acinus architecture in 3D lrECM. It was reported that Rap1 plays a role in chemokine-stimulated cell migration in lymphocytes and endothelial cells as well as bladder carcinoma cell migration (Wittchen et al. 2005). In addition, Rap1 was activated in metastatic mammary carcinoma of Crkl transgenic mice (Hemmerlyckx et al. 2001). Thus, I performed matrigel invasion assay to determine the effect of Rap1 in the invasiveness of T4-2 cells. When compared to control T4-YFP cells, T4-Rap1DA cells showed significantly ( $\sim 4$ -fold) increased invasion through matrigel-

coated transwell filters, while the invasiveness of T4-Rap1DN cells was less than half that of the controls (Figure 6A).

Next, I determined the effect of Rap1 on tumorigenic potential of T4-2 cells. Xenograft tumors were examined by injecting transfectants subcutaneously into athymic nude mice. Tumor growth *in vivo* was enhanced by the expression of dominant-active Rap1, while it was suppressed by dominant-negative Rap1 (Figure 6B). The tissue sections from 8 week tumor samples indicated that the tumors formed by control T4-YFP cells were not dividing anymore and differentiated. On the other hand, T4-Rap1DA tumors appeared to still proliferate and blood vessels were often observed (Figure 6C).

These results indicated that activation of Rap1 can promote several aspects of malignancy in breast cancer cells, while down-regulation of Rap1 has an inhibitory effect.

### **Phenotypic reversion occurs *via* a modulation of different signaling pathways than other reverting reagents**

To dissect the molecular mediators of these cellular phenotypes caused by modulation of Rap1 signaling, I analyzed the biochemical characteristics of the transfectants. Although the previous data revealed that there is a correlation between acinus architecture and the expression of EGFR,  $\beta$ 1-integrin, and PTEN in the presence or absence of inhibitors against EGFR,  $\beta$ 1-integrin, MEK, or PI3K in our model system, the expression of either of those three molecules was not altered in T4-Rap1DN spheroids, which had phenotypically reverted organized acinus architecture (Figure 7A). Furthermore, T4-Rap1DA colonies did not exhibit elevated EGFR activity despite their resistance to reversion by AG1478. Therefore, molecular mediators which influence phenotypes of Rap1 transfected T4-2 cells in 3D lrECM appeared to differ from those by modulating EGFR,  $\beta$ 1-integrin, MEK, or PI3K alone.

Several studies have reported that Rap1 affects the activity of Erk, p38, or Akt with cell-type and context dependent manner (Stork, 2003), thus the expression and phosphorylation levels of these proteins in the transfectants were determined (Figure 7B). Phospho-Erk level was greatly upregulated and phospho-Akt was slightly up-regulated in T4-Rap1DA colonies as compared to control T4-YFP colonies in 3D lrECM. In 2D cultured cells, on the other hand, the differences in either phosphorylation levels or expressions of these proteins were not detected among the transfections (data not shown). T4-Rap1DN spheroids in 3D lrECM exhibited significantly decreased Akt activity and slight reduction of Erk activity than T4-YFP colonies. The phosphorylation and expression of p38 were unaffected by expression of dominant-active or dominant-negative Rap1 in both 2D and 3D lrECM cultured T4-2 cells.

I then examined downstream of Erk and Akt pathways (Figure 7C). p90RSK, a major target of Erk involved in cell proliferation, showed higher activation in T4-Rap1DA colonies, while it was slightly down-regulated in T4-Rap1DN spheroids, as compared to T4-YFP colonies. Akt directly phosphorylates GSK3- $\beta$  and affects various cellular events. Akt also phosphorylates TSC2 and inhibits its function as a tumor suppressor. Phospho-GSK3 $\beta$  and phospho-TSC2 level was decreased in T4-Rap1DN

spheroids in a similar manner with phospho-Akt level. Recent studies revealed that TSC2 is involved in regulation of translation machinery through mTOR and increased translational signal causes tumor progression (Martin and Hall, 2005). The downstream targets of TSC2, S6 ribosomal protein and 4EBP1, were highly phosphorylated in T4-Rap1DA colonies, while they were less phosphorylated in T4-Rap1DN spheroids than T4-YFP colonies (Figure 7D). Therefore, translational pathway seemed to be more activated and inactivated by dominant-active and dominant-negative Rap1, respectively.

These results indicated that both Erk and Akt pathways were modulated by Rap1 in the context of 3D IrECM culture, but that the feedback regulation on the levels of EGFR and integrin did not occur.

**Task4: Determine gene expression profile in S1, T4-2, and reverted T4-2 cells using DNA microarray**, is an effective approach to identify candidate genes involved in organization of polarized tissue architecture. Since the analyses of 3D IrECM cultured T4-2 cells transfected with dominant-active and dominant-negative Rap1 showed that Rap1 play a role in organizing polarity and tissue architecture via coordinating several signaling pathways, I performed Task4 using T4-YFP, T4-Rap1DA, T4-Rap1DN. RNA was isolated from these cells after cultured in 3D IrECM for 10 days and hybridized with Affymetrix DNA chips spotted with 22,000 human oligos. Obtained data were processed and analyzed with GeneSpring software.

484 genes are up-regulated and 361 genes are down-regulated more than 2-fold in T4-Rap1DA cells compared to control T4-YFP cells. Among 484 up-regulated genes, 162 genes were down-regulated in T4-Rap1DN cells, which are candidate genes having a correlation with Rap1 activity in 3D IrECM culture (Figure 8A). Several cell cycle regulators such as CyclinA2, CyclinB1, and CyclinB2 were identified and confirmed their alterations by RT-PCR (Figure 8B). Interestingly, all of them are G2/M cyclins and G1/S cyclins such as CyclinD were not affected by Rap1. In addition to these G2/M cyclins, a couple of genes playing a role from G2 to M phase were up-regulated in T4-Rap1DA cells and down-regulated in T4-Rap1DN cells. A serine/threonine kinase Polo-like kinase-1 (Plk1) is one of them (Eckerdt et al.). Plk1 is expressed from G2 onwards and is degraded at the end of mitosis. Although Plk1 is already present in G2, its kinase activity is first seen at the G2/M transition and reaches peak levels during mitosis. It was suggested that CyclinB-Cdk1 functions upstream of Plk1 and activate it. Up-regulation of cell cycle regulators is connected to progression of malignancy. For example, Plk1 is overexpressed in a various types of tumors and it is shown that expression level of Plk1 coincides with poor prognosis.

On the other hand, 55 genes were up-regulated in T4-Rap1DN cells among 361 down-regulated genes in T4-Rap1DA cells (Figure 9A). Several membrane proteins (FLTR3, CD164, EphA3) of which function is related to cell adhesions are identified, although their functional role in regulating tissue architecture of 3D IrECM cultured T4-2 cells is not clarified yet. Interestingly, proapoptotic factor FoxO1 is significantly increased in T4-Rap1DN cells as compared to T4-Rap1DA cells (Figure 9B). The

proapoptotic activity of FoxO1 is mediated through the transcriptional regulation of several genes such as TRAIL, FasL, and Bim, which is a critical factor for lumen formation (Reginato et al., 2005). FoxO1 induces cell cycle arrest by transcriptional repression of positive cell cycle regulators, as well as transcriptional induction of negative cell cycle regulators such as p27 and thus FoxO1 plays a tumor suppressor like functions (Accili and Arden, 2004). Thus, downregulation and upregulation of FoxO1 in T4-Rap1DA and T4-Rap1DN cells, respectively, well correlates with their phenotype in 3D lrECM.

## **Conclusion**

To clarify molecular determinants and pathways controlling polarity in breast epithelial cells, I have investigated potential polarity regulator Rap1 using 3D lrECM cultured HMT-3522 cell models. The obtained data suggests that Rap1 coordinates Erk, PI3K/PTEN-Akt, and Rac1 pathways to control polarity as well as tissue architecture. The aberrant activation of Rap1 seems to result in unbalanced signaling of these pathways and causes exaggeration of malignancy. Recent study reveals that Rac1 is constitutively activated in cells lacking Par-3, which is one of the tight junction components and an essential for epithelial cell polarization (Itoh et al., 2001). The assembly of tight junctions is efficiently restored by a dominant-negative Rac1 mutant, indicating that Rap1 may play a role of regulating tight junctions via Rac1 (Chen and Macara, 2005). The further analyses of microarray data from Task4 would be of assistance to understand molecular mechanisms how Rap1 control tight junctions and polarity through integrating Rac1, Erk, and PI3K/PTEN-Akt pathways.

## **Reportable Outcomes**

Studies described above are supposed to be presented at minisymposium in 45<sup>th</sup> annual meeting of American Society for Cell Biology and currently being compiled into a manuscript.

## **References**

- Accili D and Arden KC. (2004). FoxOs at the crossroads of cellular metabolism, differentiation, and transformation. *Cell* 117(4):421-6.
- Chen X and Macara IG. (2005). Par-3 controls tight junction assembly through the Rac exchange factor Tiam1. *Nat Cell Biol.* 7(3):262-9.
- Debnath J, Mills KR, Collins NL, Reginato MJ, Muthuswamy SK, and Brugge JS. (2002) The role of apoptosis in creating and maintaining luminal space within normal and oncogene-expressing mammary acini. *Cell* 111(1):29-40.

Eckerdt F, Yuan J, and Strebhardt K. (2005). Polo-like kinases and oncogenesis. *Oncogene*. 24(2):267-76.

Hemmeryckx B, van Wijk A, Reichert A, Kaartinen V, de Jong R, Pattengale PK, Gonzalez-Gomez I, Groffen J, and Heisterkamp N.(2001). Crkl enhances leukemogenesis in BCR/ABL P190 transgenic mice. *Cancer Res*. 61(4):1398-405.

Itoh M, Sasaki H, Furuse M, Ozaki H, Kita T, and Tsukita S. (2001). Junctional adhesion molecule (JAM) binds to PAR-3: a possible mechanism for the recruitment of PAR-3 to tight junctions. *J Cell Biol*. 154(3):491-7.

Itoh M and Bissell MJ. (2003). The organization of tight junctions in epithelia: implications for mammary gland biology and breast tumorigenesis. *J Mammary Gland Biol Neoplasia*. 8(4):449-62.

Liu H, Radisky DC, Wang F, and Bissell MJ. (2004). Polarity and proliferation are controlled by distinct signaling pathways downstream of PI3-kinase in breast epithelial tumor cells. *J Cell Biol*. 164(4):603-12.

Martin DE and Hall MN. (2005). The expanding TOR signaling network. *Curr Opin Cell Biol*. 17(2):158-66.

Reginato MJ, Mills KR, Becker EB, Lynch DK, Bonni A, Muthuswamy SK, and Brugge JS. (2005). Bim regulation of lumen formation in cultured mammary epithelial acini is targeted by oncogenes. *Mol Cell Biol*. 25(11):4591-601.

Stork PJ. (2003). Does Rap1 deserve a bad Rap? *Trends Biochem Sci*. 28(5):267-75.

Wang F, Weaver VM, Petersen OW, Larabell CA, Dedhar S, Briand P, Lupu R, and Bissell MJ. (1998). Reciprocal interactions between beta1-integrin and epidermal growth factor receptor in three-dimensional basement membrane breast cultures: a different perspective in epithelial biology. *Proc Natl Acad Sci U S A*. 95(25):14821-6.

Weaver VM, Petersen OW, Wang F, Larabell CA, Briand P, Damsky C, and Bissell MJ. (1997). Reversion of the malignant phenotype of human breast cells in three-dimensional culture and in vivo by integrin blocking antibodies. *J Cell Biol*. 137(1):231-45.

Wittchen ES, van Buul JD, Burridge K, and WorthyLake RA. (2005). Trading spaces: Rap, Rac, and Rho as architects of transendothelial migration. *Curr Opin Hematol*. 12(1):14-21.

## **Appendices**

### **Figure legends**

**Figure 1. Activity of Rap1 is up-regulated in malignant T4-2 cells compared to non-malignant S1 cells in 3D IrECM.**

Morphology and Rap1 expression/activity in non-malignant S1 and malignant T4-2 cells. (A) Phase-contrast images of S1 and T4-2 cells cultured in 3D IrECM. Bar. A comparison of the expression and activity of Rap1 between S1 and T4-2 cells. Pull-down assay for GTP-bound Rap1 revealed that Rap1 was more activate in 3D IrECM cultured malignant human breast epithelial cells. (B) YFP, YFP-tagged dominant-active Rap1, and YFP-tagged dominant-negative Rap1 were introduced into T4-2 cells. Cells were stained with anti-GFP antibody.

**Figure 2. T4-2 cells transfected with dominant-negative Rap1 exhibit reverted phenotypes in 3D IrECM.**

(A) Morphology and polarity of T4-YFP, T4-Rap1DN, and AG1478-treated T4-YFP cells in 3D IrECM. Cell polarity was examined by staining with antibodies against  $\alpha$ 6-integrin (basal),  $\beta$ -catenin (basolateral), and GM130 (apical). (B, C) Cell proliferation in 3D IrECM was determined by measuring colony size (B) and Ki-67 positive colonies (C).

**Figure 3. Lumen formation is induced in 3D IrECM cultured T4-2 cells transfected with dominant-negative Rap1, and not in AG1478-treated control.**

(A, B) After 15 days culture in 3D IrECM, lumen formation was observed in T4-Rap1DN spheroids (B), while T4-YFP cells reverted with AG1478 did not show lumen (A). (C) Distribution of actin filaments. Actin filaments were localized at apical membrane area in 3D IrECM cultured T4-Rap1DN spheroids. (D) The active-caspase3 positive apoptotic cells were detected in T4-Rap1DN cells, and not in AG1478 treated T4-YFP cells.

**Figure 4. T4-2 cells transfected with dominant-active Rap1 are resistant to reversion by normal concentration of AG1478.**

(A) Morphology and polarity of T4-Rap1DA and AG1478-treated T4-Rap1DA colonies in 3D IrECM. Colonies were stained with anti- $\alpha$ 6-integrin, anti- $\beta$ -catenin, and anti-GM130 antibodies. (B, C) Comparison of cell proliferation between T4-Rap1DA and AG1478-treated T4-Rap1DA colonies. Unlike control T4-YFP colonies, size (B) or Ki-67 positive ratio (C) of T4-Rap1DA colonies was not affected by treatment with normal concentration of AG1478 (70nM). (D) The effect of AG1478 treatment on  $\beta$ 1-integrin, EGFR, and PTEN in T4-YFP and T4-Rap1DA colonies. Expression of  $\beta$ 1-integrin and EGFR, and phospho-EGFR was reduced, while PTEN expression was up-regulated in AG1478-treated T4-YFP colonies but not in AG1478-treated T4-Rap1DA colonies.

**Figure 5. Dose dependent effects of inhibitors on T4-Rap1DA colonies.**

Cells were treated with different dose of inhibitors against EGFR (A; AG1478 and B; mAb225), MEK (C; PD98059) or PI3K (D; LY294002). T4-Rap1DA colonies showed reverted phenotype when concentration of inhibitors against EGFR and MEK was increased 3-fold higher than normal concentration required to revert control T4-YFP

colonies, while almost same concentration of LY294002 was able to revert both T4-YFP and T4-Rap1DA colonies.

**Figure 6. Level of Rap1 activity regulates cell tumorigenesis and invasive phenotype**  
(A) Cell invasiveness is altered by Rap1 mutant. Up-regulation of Rap1 increased, while down-regulation of Rap1 reduced invasion of T4-2 cells. (B) T4-2 transfectants were subcutaneously injected into nude mice. T4-Rap1DA cells exhibited enhanced tumorigenicity, whereas T4-Rap1DN cells almost lost it compared to control T4-YFP cells. (C) Histology of tumors derived from T4-YFP and T4-Rap1DA cells.

**Figure 7. Phenotypic alteration by Rap1 activity occurs through different signaling pathways from a modulation of EGFR or  $\beta$ 1-integrin.**

Erk and Akt pathways were affected in Rap1 mutant transfected T4-2 cells in 3D IrECM. Expression and/or phosphorylation of (A)  $\beta$ 1-integrin, EGFR, and PTEN; (B) possible signaling molecules affected by Rap1; (C) downstream targets of ERK and AKT; (D) downstream translational signaling molecules were affected by Rap1.

**Figure 8. Genes up-regulated by dominant-active Rap1 and down-regulated by dominant-negative Rap1 in 3D IrECM cultured T4-2 cells.** (A) RNA was isolated from 3D IrECM cultured T4-Rap1DA, and T4-Rap1DN cells for 10days. Isolated RNA was labeled and hybridized with Affymetrix human DNA oligo chips. Genes up-regulated more than 2-fold in T4-Rap1DA and down-regulated more than 2-fold in T4-Rap1DN cells as compared to T4-YFP cells were chosen. (B) Expression of cell cycle regulator genes in the list were analyzed by RT-PCR.

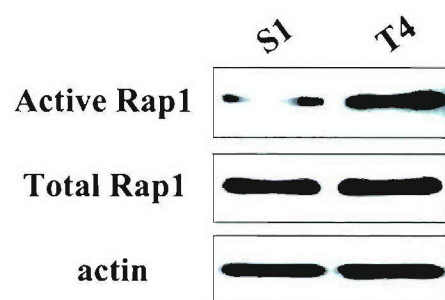
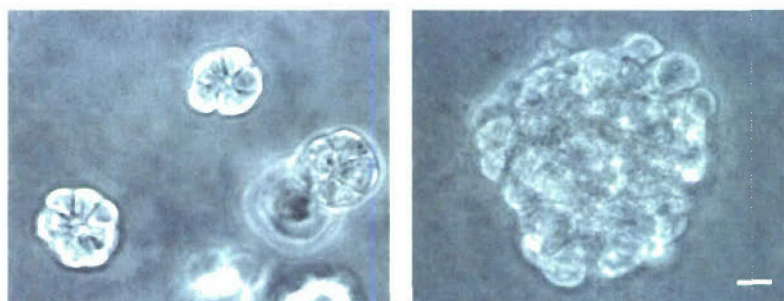
**Figure 9. Genes down-regulated by dominant-active Rap1 and up-regulated by dominant-negative Rap1 in 3D IrECM cultured T4-2 cells.** (A) From the same data set in figure 8, genes down-regulated more than 2-fold in T4-Rap1DA and up-regulated more than 2-fold in T4-Rap1DN cells as compared to T4-YFP cells were chosen. (B) The array data was validated by RT-PCR regarding couple of adhesion related molecules (FLRT3, CD164, EphA3) and proapoptotic molecule FoxO1.

**A**

**3D IrECM**

**S1**

**T4-2**



**B**

**T4-YFP**

**T4-Rap1DA**

**T4-Rap1DN**

**YFP**



**Figure 1**

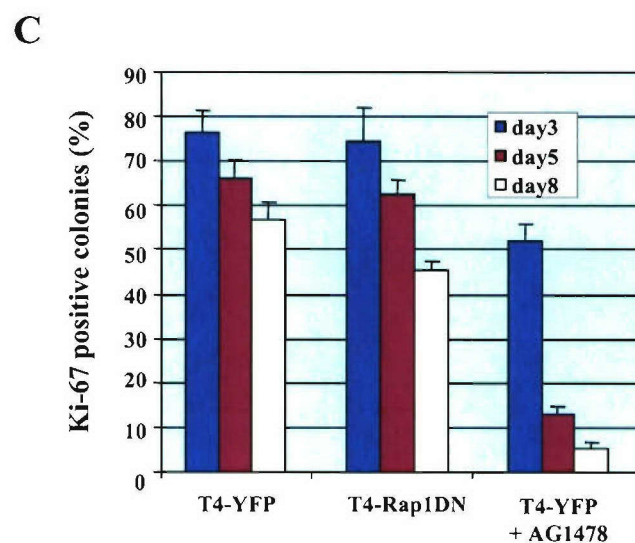
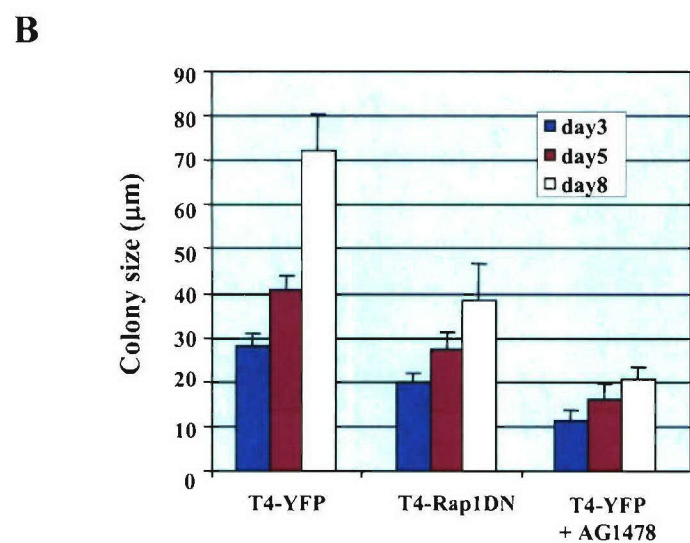
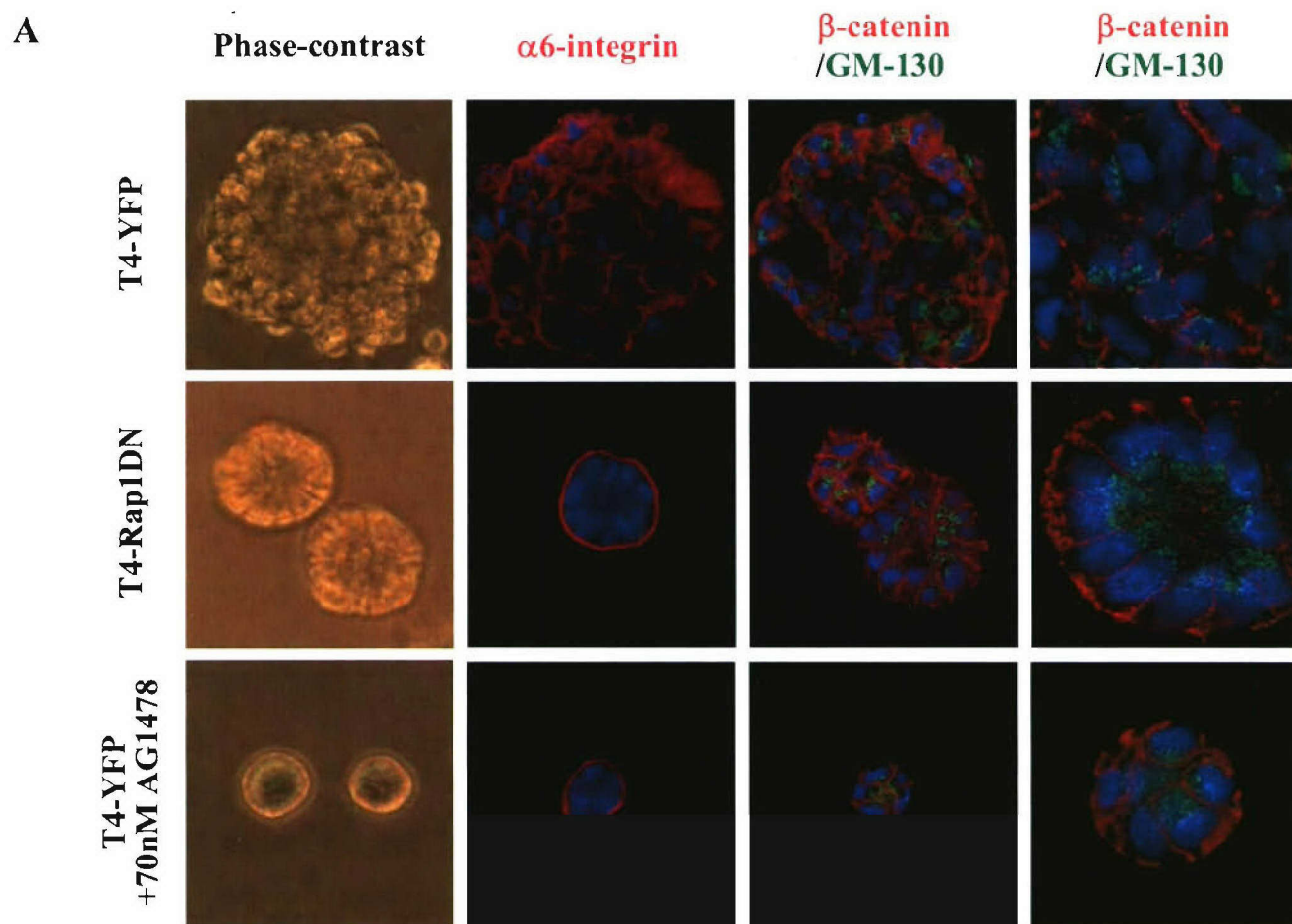
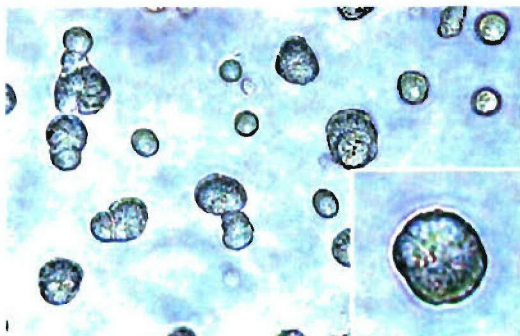


**Figure 2**

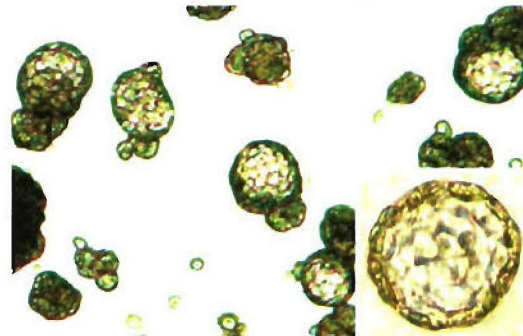
A

T4-YFP (+AG1478) day15



B

T4-Rap1DN day15



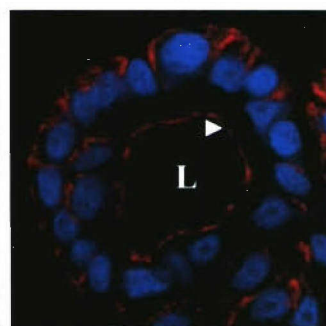
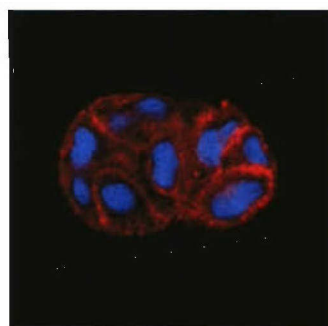
C

day15

T4-YFP (+AG1478)

T4-Rap1DN

actin



D

day10

T4-YFP (+AG1478)

T4-Rap1DN

active-Casp3

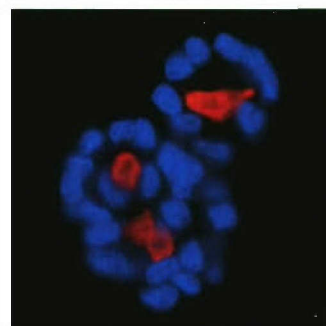
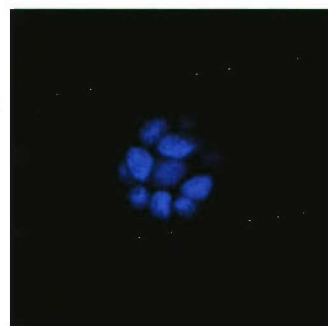
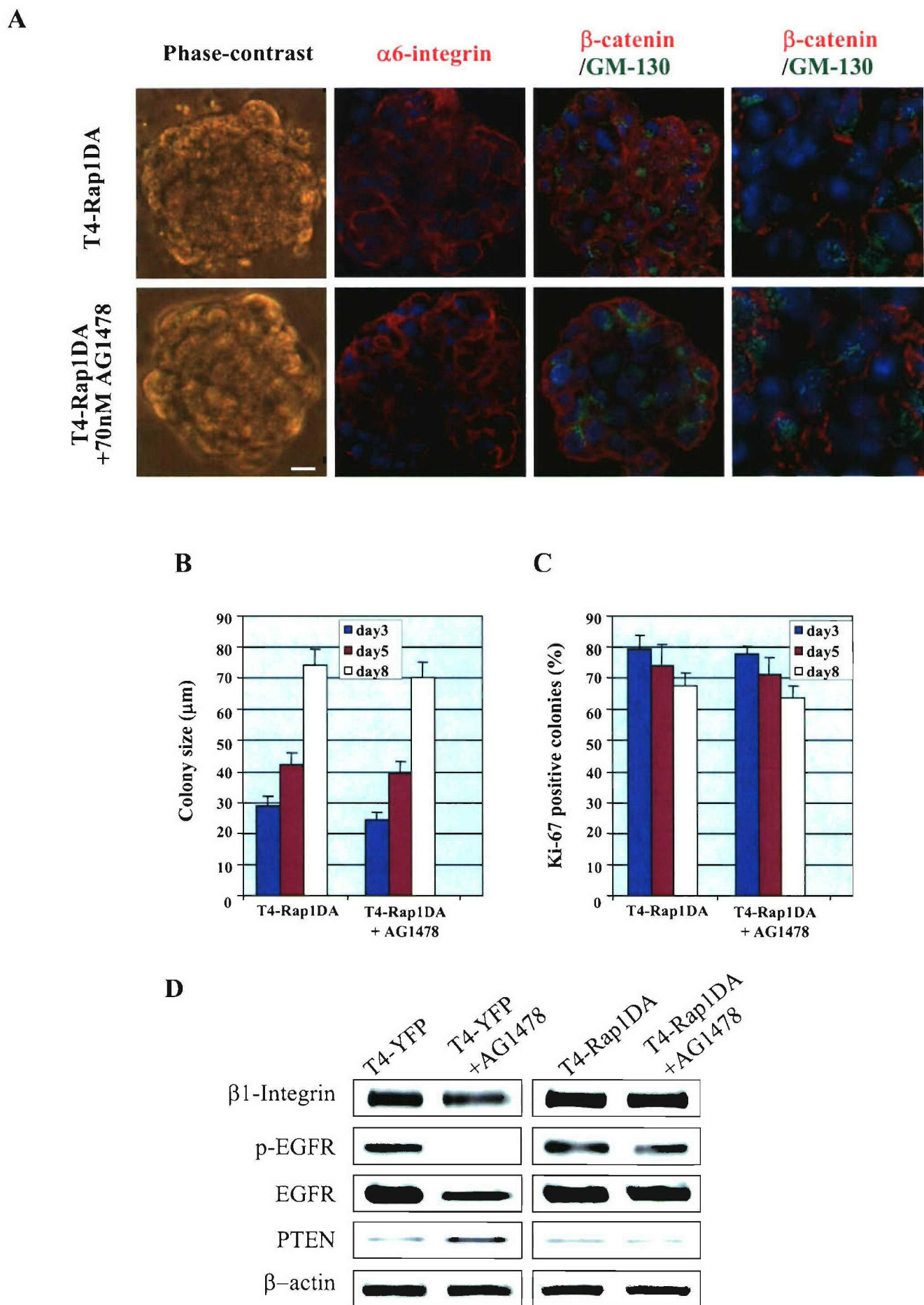
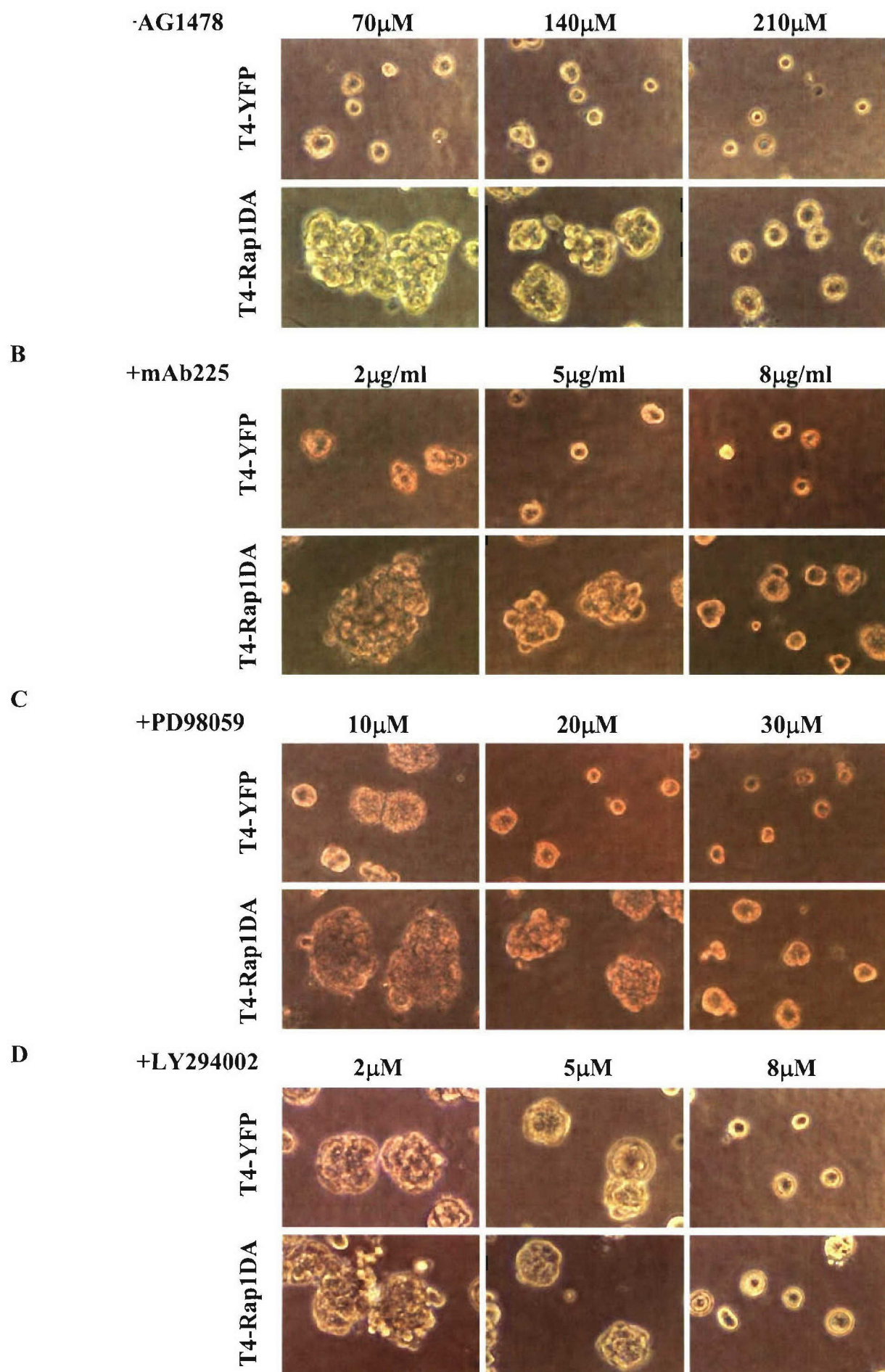


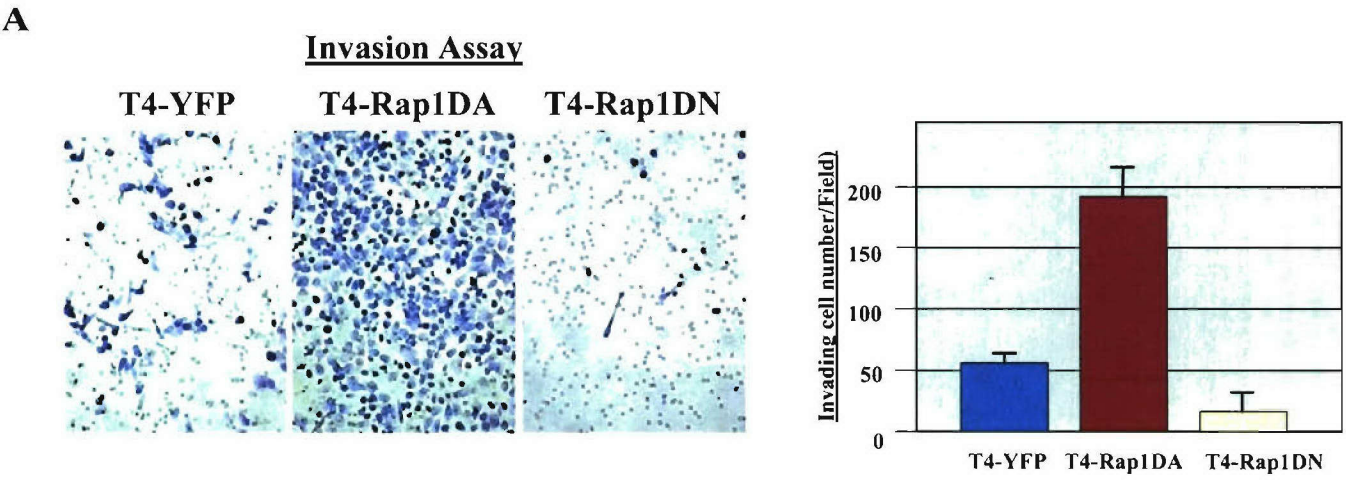
Figure 3



**Figure 4**



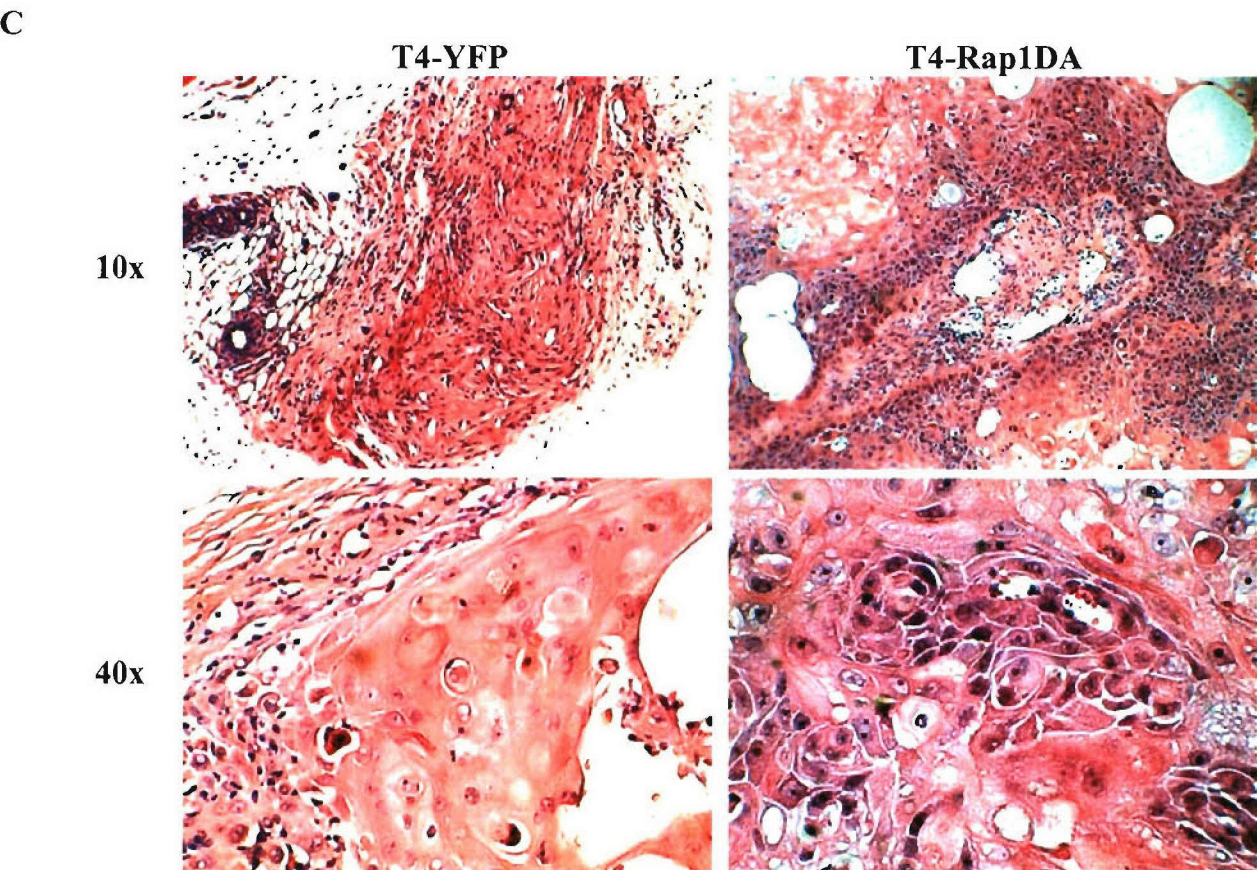
**Figure 5**



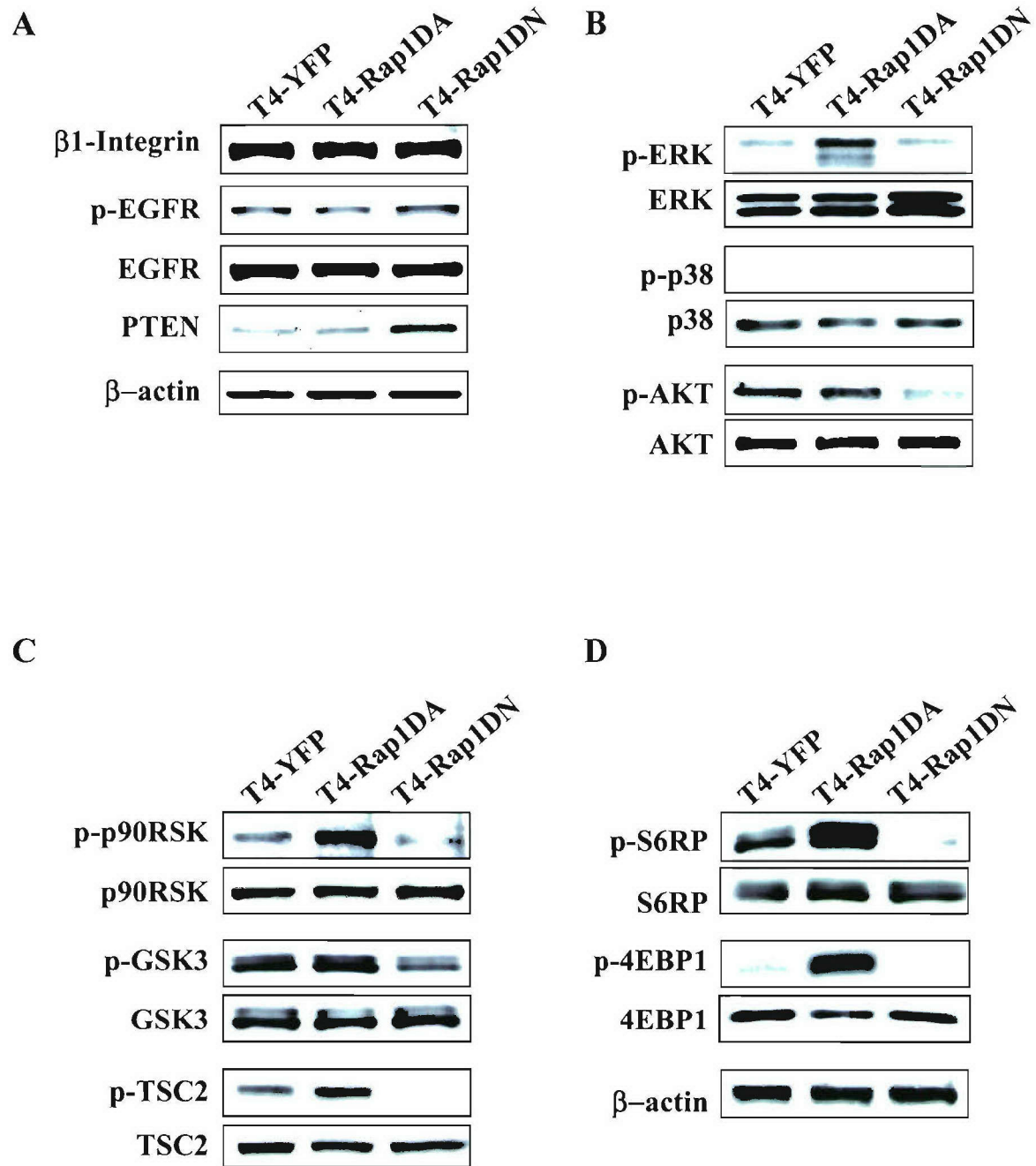
**B**

**Tumorigenicity of Rap1 transfectants**

Injected cells	Total number of tumors per group	Tumor size		
		> 10 mm <sup>3</sup> tumors	< 10 mm <sup>3</sup> tumors	Mice with no tumors
T4-YFP	8/8	5/8	3/8	0/8
T4-Rap1DA	8/8	8/8	0/8	0/8
T4-Rap1DN	2/8	1/8	1/8	6/8



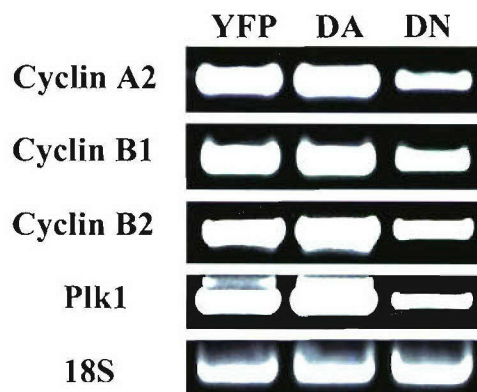
**Figure 6**



**Figure 7**

**A**

Gene	Relative Expression			Tentative Functions
	YFP	Rap1DA	Rap1DN	
CCNA2	1.0919973	2.6425416	0.053592324	cytokinesis; mitosis; mitotic G2 checkpoint
TYMS	0.5480279	1.4277822	0.036987495	
MKI67	0.8552262	2.5746226	0.06579376	
HCAP-G	1.0215628	2.4948568	0.078790754	
BUB1	0.9244152	2.0006654	0.07384517	cell cycle; mitosis; mitotic spindle checkpoint
BIRC5	0.5966417	1.8545531	0.048084654	
DLG7	0.82783484	2.305587	0.070864715	cell-cell signaling
CCNB2	0.87147295	2.120064	0.08310534	cytokinesis; mitosis; regulation of cell cycle
ITGB6	1.5257393	3.8000565	0.15119849	cell-matrix adhesion; integrin-mediated signaling pathway
KIF23	0.63200533	2.0384495	0.06445863	
PRC1	0.85922474	1.858448	0.088264965	
RAMP	0.4417453	1.1165247	0.0488256	
HMMR	0.872858	2.1214485	0.10348793	cell motility
KIF2C	1.1181177	2.410515	0.1351367	cell proliferation; mitosis
HCD	0.816046	2.2311494	0.09981128	
FOXM1	0.6544714	1.7568898	0.08130836	regulation of transcription, DNA-dependent; protein amino acid phosphorylation
TOPK	0.5345668	1.2398124	0.06750798	
SHCBP1	0.7688209	1.8113261	0.09726562	cytokinesis; meiosis
NEK2	0.9043545	1.8563162	0.115533575	
CENPA	1.0519868	2.146762	0.13443993	
BUB1B	0.748842	1.8407941	0.0959621	
BM039	1.0119541	2.5257983	0.13072856	cell cycle; mitosis; mitotic checkpoint
TTK	0.6439535	1.7277372	0.08524491	
NUSAP1	0.63831764	1.4323531	0.08451068	
ITGB6	1.2261727	2.9842029	0.16436659	
TOP2A	0.6450744	1.5723388	0.08753789	cell-matrix adhesion; integrin-mediated signaling pathway
CDC20	0.9665929	2.0321836	0.13187684	
CCNB1	0.8328396	2.0190184	0.11442966	
KIF2C	1.0239981	2.1265752	0.14333156	
TOP2A	0.6239979	1.5876833	0.08759065	cytokinesis; mitosis; regulation of cell cycle;
KIF14	0.83382434	2.1153696	0.11708649	
MELK	0.9382825	2.3146737	0.13383737	
PLK1	0.86326206	2.5722015	0.12395659	

**B****Figure 8**

A	Gène	Relative Expression			Tentative Functions
		YFP	Rap1DA	Rap1DN	
	FLRT3	0.790824	0.103422	1.6006106	cell adhesion
	FOXO1A	0.4757368	0.0796958	1.4303746	cell growth and/or maintenance
	FOXO1A	0.4925211	0.0933921	1.3289582	
	SSBP2	0.6277085	0.1281728	1.2609769	regulation of transcription
	SFTPD	0.36057106	0.08233767	6.842762	alveolus development; antimicrobial humoral response
	CHI3L1	0.71042913	0.16271149	12.270392	metabolism
	GLUL	0.92143136	0.21382467	2.0767071	glutamine biosynthesis; regulation of neurotransmitter levels
	PIK3R1	0.85376036	0.19904014	1.9414734	
	EDN2	0.90809673	0.25050837	2.0687683	cell-cell signaling; pathogenesis; protein kinase C activation
	ZNF117	1.385492	0.42278636	3.9010868	regulation of transcription, DNA-dependent
	CHI3L1	0.7882396	0.24171974	13.36809	metabolism
	PIK3R1	0.9270732	0.2915556	2.3769877	
	BTN3A3	1.2455647	0.39832592	3.2908442	
	DHRS3	1.1043123	0.35417378	2.4478369	fatty acid metabolism; visual perception
	PIK3R1	0.8676907	0.28249344	2.1894214	
	ZNF145	0.4386975	0.14296351	1.9047638	cell growth and/or maintenance; mesoderm development
	SATB1	0.98099995	0.3377764	3.154174	establishment and/or maintenance of chromatin architecture
	SAH	1.9256705	0.66484934	3.890238	
	H15535	0.5413008	0.18692802	1.3262423	
	LIMK2	0.91330034	0.317773	3.498192	
	PLSCR4	0.7949644	0.28097877	2.6874092	blood coagulation; phospholipid scrambling
	CYBRD1	0.9787124	0.35122323	3.3442028	electron transport
	MGC5618	1.323369	0.4926617	3.7010477	
	GBP2	0.527534	0.19711149	3.625249	immune response
	CFLAR	1.4059851	0.52652043	2.9176702	induction of apoptosis by extracellular signals;
	CFLAR	1.3396767	0.50927955	2.9352493	induction of apoptosis by extracellular signals
	LIMK2	1.2721328	0.4895091	4.924092	
	BTN3A3	1.1174442	0.43154046	3.293279	
	CFLAR	1.2953199	0.50313205	3.1971414	induction of apoptosis by extracellular signals
	SOD2	1.8470949	0.7515606	4.305439	response to oxidative stress; superoxide metabolism
	IFIT1	0.7861041	0.32023448	3.48812	immune response
	RNASE4	1.0720158	0.4436017	2.2065537	
	EFEMP1	0.322507	0.13526835	2.5287693	visual perception

## B

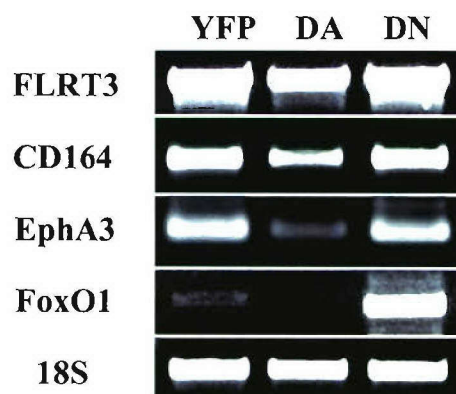


**Figure 9**